

# Using Effusive Molecular Beams and Microcanonical Unimolecular Rate Theory to Characterize CH<sub>4</sub> Dissociation on Pt(111)

Kristy M. DeWitt, Leticia Valadez, Heather L. Abbott, Kurt W. Kolasinski, and Ian Harrison\*

Department of Chemistry, University of Virginia, Charlottesville, Virginia 22904-4319

Received: November 18, 2005; In Final Form: February 3, 2006

The dissociative sticking coefficient for CH<sub>4</sub> on Pt(111) has been measured as a function of both gas temperature ( $T_g$ ) and surface temperature ( $T_s$ ) using effusive molecular beam and angle-integrated ambient gas dosing methods. The experimental results are used to optimize the three parameters of a microcanonical unimolecular rate theory (MURT) model of the reactive system. The MURT calculations allow us to extract transition state properties from the data as well as to compare our data directly to other molecular beam and thermal equilibrium sticking measurements. We find a threshold energy for dissociation of  $E_0 = 52.5 \pm 3.5$  kJ mol<sup>-1</sup>. Furthermore, the MURT with an optimized parameter set provides for a predictive understanding of the kinetics of this C–H bond activation reaction, that is, it allows us to predict the dissociative sticking coefficient of CH<sub>4</sub> on Pt(111) for any combination of  $T_s$  and  $T_g$  even if the two are not equal to one another, indeed, the distribution of molecular energy need not even be thermal. Comparison of our results to those from recent thermal equilibrium catalysis studies on CH<sub>4</sub> reforming over Pt nanoclusters (~2 nm diam) dispersed on oxide substrates indicates that the reactivity of Pt(111) exceeds that of the Pt nanocatalysts by several orders of magnitude.

## Introduction

Methane, found in natural gas and methane hydrates, is the most abundant hydrocarbon natural resource. Nevertheless, the exploitation of methane for energy and as a chemical feedstock is hampered by the need to liquefy the gas prior to transport as well as the large energy of activation, which hinders the transformation of CH<sub>4</sub> into more valuable chemicals. The prime industrial source of hydrogen is steam reforming of CH<sub>4</sub> to produce syngas (H<sub>2</sub> + CO). Syngas is also the starting material for Fischer–Tropsch synthesis of higher order hydrocarbons. These are some of the factors that lend C–H bond activation its technical importance and have led to a significant body of work on catalytic C–H bond activation.<sup>1–3</sup> More efficient catalysts for the dissociation of CH<sub>4</sub> are required to improve steam reforming and to make the production of H<sub>2</sub> less expensive. We report results here which show that nanoscale catalysts underperform flat single-crystal surfaces by several orders of magnitude and that, therefore, considerable headroom for improvement of industrial processes may exist.

Our understanding of reactivity at the gas/surface interface has increased greatly in recent years.<sup>4</sup> Molecular beam techniques,<sup>5,6</sup> especially when coupled with laser detection,<sup>7</sup> have been particularly important in the development of this understanding. The activation of the C–H bond in CH<sub>4</sub> is no exception to this. Molecular beam experiments, particularly at high translational energy, have been reviewed by Weaver, Carlsson, and Madix.<sup>8</sup> The groups of Utz<sup>9–11</sup> and Beck<sup>12–14</sup> have recently explored the quantum state specificity of the dissociation reaction. Nonetheless, what these supersonic molecular beam studies and related dynamical theories have failed to provide is a predictive understanding of the reactivity of CH<sub>4</sub> at a surface. That is, while these dynamical studies have identified instances of mode-selective chemistry and that the

dissociative sticking scales with the normal component of the CH<sub>4</sub> translational energy, they are still unable to answer some very fundamental questions such as: (i) For a given metal surface, for example, Pt(111), what is the dissociative sticking coefficient when gas at a temperature  $T_g = x$  impinges on a surface at temperature  $T_s = y$ , and (ii) what are the characteristics of the reactive transition state (e.g., dissociation threshold energy, vibrational frequencies, etc.) that could be compared with the results of electronic structure theory calculations? Here, we illustrate how relatively easy-to-implement effusive molecular beam experiments in conjunction with microcanonical unimolecular rate theory (MURT) analysis can be used to address these fundamental questions.

The number of models to explain the dynamics of CH<sub>4</sub> dissociation on metal surfaces is almost as great as the number of groups that have studied the problem. Winters<sup>15,16</sup> and Rettner et al.<sup>17</sup> investigated W surfaces. Ehrlich and co-workers studied Rh<sup>18–20</sup> as well as W surfaces.<sup>21</sup> Madix and co-workers have investigated Ni, Ir, Pd, and Pt.<sup>8,22–25</sup> Ir and Rh have been investigated by Weinberg and co-workers.<sup>26–33</sup> Ir has also been studied by Mullins and co-workers.<sup>34–36</sup> Molecular beam work has been performed in Ceyer's lab<sup>37–40</sup> on Ni, which has also been studied in thermal experiments by Goodman and co-workers.<sup>41,42</sup> Chorkendorff and co-workers<sup>1,43–45</sup> have studied Ni and Ru surfaces with molecular beam and thermal techniques. Luntz and co-workers have concentrated mainly on Pt(111)<sup>46–51</sup> but also Pt(110)<sup>52</sup> whereas King and co-workers have studied Pt(110).<sup>53,54</sup> A substantial kinetic isotope effect, that is, a lower dissociative sticking coefficient for CD<sub>4</sub> compared with CH<sub>4</sub>, has been observed and has often been cited to invoke a quantum mechanical tunneling mechanism, though this is not universally accepted.<sup>21,31,55</sup> Generally, translational energy increases sticking except for low energies on Ir(111),<sup>36</sup> Ir(110),<sup>34,35</sup> and Pt(110).<sup>53</sup> Likewise, vibrational energy always enhances sticking apart from a narrow range of kinetic energies for some vibrational modes on Pt(110).<sup>53</sup> Increasing  $T_s$  increases dissociative sticking

\* To whom correspondence should be addressed. Fax: (434) 924-3966. Tel: (434) 924-3639. E-mail: harrison@virginia.edu.

although the effect may be imperceptible under some experimental conditions when the reactivity is already high.

Winters suggested a model for W surfaces involving tunneling from a vibrationally excited molecule bound in an equilibrated precursor state.<sup>16</sup> Rettner et al.<sup>17</sup> demonstrated unequivocally the strong dependence of the sticking coefficient on translational and vibrational excitation and posited that translationally activated tunneling through a one-dimensional (1D) barrier explained their molecular beam data. Ehrlich and co-workers<sup>18,20</sup> proposed that sticking on Rh surfaces is controlled by a complicated combination of direct dissociation, thermally activated precursor mediated dissociation, and a hot precursor mechanism. On Ni, Lee et al.<sup>38</sup> invoked vibrational excitation and direct translation–vibration energy transfer to facilitate angular deformation as the crucial step in dissociation (the “splat” mechanism). They argued against tunneling as being the sole contributor to the observed isotope effect but suggested that it might make some contribution. On Ir(110)–(2 × 1), Seets et al.<sup>34</sup> argue in favor of a combination of precursor mediated trapping/dissociation at low translational energy with direct dissociation at high energy. Having discarded their earlier model,<sup>53</sup> King and co-workers<sup>54</sup> support a similar combination of dynamical channels on Pt(110)–(2 × 1). Goodman and co-workers<sup>41,42</sup> and Chorkendorff and co-workers<sup>43,45</sup> agree that a direct channel dominates on Ni(111), and the latter group has shown that a direct pathway rather than a precursor mediated one is important for Ni(100) under conditions appropriate to industrial steam reforming of CH<sub>4</sub>. Luntz, Harris, and co-workers<sup>46–52</sup> argue that, while precursors may be important for heavier alkanes, direct dissociation dynamics rules the day for CH<sub>4</sub>. Regardless of whether tunneling is involved in crossing the barrier or not, their work demonstrates unequivocally that a surface temperature-dependent sticking coefficient is not an unambiguous signature of a precursor mediated mechanism because the motion of surface atoms and phonon states strongly influences energy exchange even in a direct mechanism. Therefore, apart from Ir(111), Ir(110)–(2 × 1), and Pt(110)–(2 × 1) at low translational energies, CH<sub>4</sub> dissociation is direct and is enhanced by higher kinetic and vibrational energy as well as by increased  $T_s$ ; however, the degree of activation varies from one metal surface to the next.

Vibrational energy enhances the reactive sticking coefficient of CH<sub>4</sub> on Ni<sup>9–14,38,43,44</sup> and Pt<sup>51,56</sup> surfaces. Interestingly, vibrational energy may be less or more efficient at increasing reactivity than is a comparable amount of translational energy. The vibrational efficacy  $\eta_v$ , essentially the factor relating how well vibrational energy in specific modes enhances reactivity compared with translational energy, is used to quantify this relationship. For CH<sub>4</sub>, which has a variety of vibrational modes, some efficacies have been measured by the groups of Utz<sup>9–11</sup> on Ni(100) and Ni(111), Beck<sup>12–14</sup> on Ni(100), and Bernasek<sup>56</sup> on Pt(111). It is found that  $\eta_v(1\nu_3) = 1$ ,  $\eta_v(2\nu_3) = 1$ ,  $\eta_v(1\nu_1) = 1.4$ , and  $\eta_v(3\nu_4) < 0.7$  (though not yet fully characterized) on Ni(100), whereas on Ni(111),  $\eta_v(1\nu_3) = 1.25$  and  $\eta_v(3\nu_4) = 0.72$ . The average of these vibrational efficacies on the Ni surfaces is  $\bar{\eta}_v \approx 1$ . On Pt(111), only  $\eta_v(2\nu_3) = 0.42$  has been measured.

Interpretation of vibrational efficacy is ambiguous.<sup>57,58</sup> First,  $\eta_v$  might not be a constant but may vary with other parameters such as the translational energy and  $T_s$ . This should be particularly pronounced for translational energies near the dissociation threshold energy. Second, to determine whether efficacy parameters have a bearing on the observation of mode-specific chemistry, the efficacies of various degrees of freedom

must be evaluated for collision complexes of the same total energy  $E^*$  (defined below) as was done successfully by Beck et al.<sup>13,14</sup> Nonetheless, variations in efficacy from one mode to the next, above and below  $\eta_v = 1$  (the prior expectation for statistical theories of reactivity), may balance out such that, once averaged over a thermal distribution, the variation may have an inconsequential influence on the overall reaction kinetics.

Not all forms of energy are equally effective at promoting chemical reactions, and it is the topology of the potential energy hypersurface (PES) that determines the relative efficacies of each mode. This is embodied in the Polanyi rules.<sup>59–61</sup> Ever since this recognition of the role of the PES, mode-selective chemistry has been something of a Holy Grail in chemical physics<sup>62,63</sup> and there is experimental evidence for it in the gas-phase reactions of methane.<sup>64,65</sup> While the results of Utz, Beck, and co-workers present us with clear evidence for mode-selective chemistry, they do not give us a method to evaluate its importance for arbitrary surface and gas temperatures. Our objective here is to determine to what extent a statistical theory can be used to predict reaction rates for arbitrary combinations of gas and surface temperature, to quantify to what extent mode-selective behavior leads to deviation from statistical behavior, and to show how far thermal effusive molecular beams in combination with a statistical theory can advance a quantitative understanding of dissociative chemisorption.

Rettner et al.<sup>66</sup> argued that a sigmoidal shape is expected to describe a state-resolved initial sticking coefficient  $S$  if a Gaussian distribution of barrier heights centered about a mean value  $E_0(v, J)$  is encountered by the molecule incident on the surface. Harris<sup>67</sup> latter suggested a tanh function to describe this shape, but Michelsen et al.<sup>68</sup> determined that the sticking coefficient data of numerous molecular beam experiments was better fitted by a state-resolved sticking function containing an error function according to

$$S(E_t, \vartheta, v, J, T_s) = \frac{A(v, J)}{2} \left[ 1 + \operatorname{erf} \left( \frac{E_n - E_0(v, J)}{W(v, J, T_s)} \right) \right] \quad (1)$$

in which  $S$  depends on the translational energy  $E_t$ , which with the angle of incidence  $\vartheta$  determines the normal energy according to

$$E_n = E_t \cos^2 \vartheta \quad (2)$$

Normal energy scaling for the dissociation of CH<sub>4</sub> on Pt(111) has been confirmed by supersonic molecular beam experiments.<sup>51</sup>  $S$  also depends on  $T_s$  and the rovibrational quantum numbers  $v$  and  $J$ .  $A(v, J)$  is the saturation sticking coefficient.  $E_0(v, J)$  is the normal translational energy at the center point of the sigmoidal  $S(E_n)$  curve and is often estimated to be the mean threshold energy for dissociation of the  $(v, J)$  rovibrational state. Both  $A(v, J)$  and  $E_0(v, J)$  appear to depend on  $v$ , probably on  $J$ , and  $A(v, J)$  may also have a  $T_s$  dependence. The width of the barrier distribution  $W$  depends on  $v$ ,  $J$ , and  $T_s$  and is empirically defined in terms of the range of barriers presented by impact at various molecular orientations at different points in the surface unit cell. Luntz<sup>69</sup> has presented a derivation of eq 1 that gives it justification beyond the empirical, in which  $W$  is defined as the sum of two terms: one representing the range of barriers and a second representing a distribution in energy transfer to the lattice. However, the correspondence between  $E_0(v, J)$  values derived from fits to eq 1 for H<sub>2</sub>/Cu and the transition state barrier height derived from *ab initio* calculations may be fortuitous because analysis of vibrationally resolved CH<sub>4</sub>/Ni sticking data

does not reveal a similar level of agreement.<sup>58</sup> Thus, a full dynamical description of the dissociative sticking within this type of model demands knowing three parameters (at least one of which has a  $T_s$  dependence of arbitrary form) *for each quantum state of the molecule*.

In a thermal bulb experiment only two parameters are derived from an Arrhenius analysis, denoted  $E_a$  and  $A$  though the preexponential factor  $A$  here has a different meaning than  $A(\nu, J)$  above. In addition, it should be noted that  $E_a$  is related to but not equal to the reaction threshold energy  $E_0$  of transition state theory.<sup>57</sup> The bulb experiment delivers no dynamical information as to which degrees of freedom are important for reaction and allows no prediction to be made for dissociative sticking under nonequilibrium circumstances. Hence, there is a driving need to perform molecular beam experiments to gain insight into the reaction dynamics and the underlying PES. In a fully state-resolved supersonic molecular beam experiment, at least six variables ( $\langle E_t \rangle$ , the translational temperature  $T_t$ ,  $\vartheta$ ,  $\nu$ ,  $J$ , and  $T_s$ , seven if the azimuthal angle  $\varphi$  is included) must be specified and such experiments provide opportunities to identify the roles of molecular degrees of freedom with great precision. For prediction of dissociative sticking coefficients using a dynamical description, however, these specified variables yield three parameters [ $A(\nu, J)$ ,  $E_0(\nu, J)$ , and  $W(\nu, J, T_s)$ ] and (if we are fortunate) the functional form of their  $T_s$  dependence for *each* quantum state. Sticking calculations can be made for either equilibrium or nonequilibrium conditions, but we require a virtual phonebook of parameters (a minimum of 3 times the number of relevant quantum states) for each  $T_s$ .

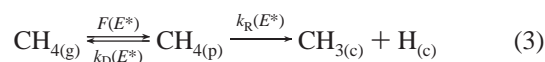
One of the reasons for the proliferation of models to describe CH<sub>4</sub> dissociation dynamics is that they only allow for quantitative predictions over very limited ranges of experimental data, if at all. Bukoski, Blumling, and Harrison<sup>57</sup> demonstrated that a three-parameter MURT can *quantitatively* describe the supersonic molecular beam sticking data of Luntz and co-workers for CH<sub>4</sub> and CD<sub>4</sub> on Pt(111).<sup>50,51</sup> Therefore, the dynamics described in the MURT model must contain the essence of the dissociation dynamics of methane on Pt(111). Similarly, good quantitative descriptions have since been demonstrated for methane/Ni(100),<sup>58,70,71</sup> CH<sub>4</sub>/Ir(111),<sup>72</sup> and SiH<sub>4</sub>/Si(100).<sup>73</sup> Worth pointing out is that extraction of the CH<sub>4</sub>/Ni(100) MURT parameters from excellent fits to the high signal-to-noise ( $2\nu_3$ ,  $J = 2$ ) eigenstate resolved and heated nozzle molecular beam data of Beck et al.<sup>12</sup> led directly to accurate (ca.  $\pm 33\%$ ) predictions of the Nielsen et al.<sup>45</sup> thermal bulb sticking at millibar pressures without resorting to any kind of data scaling.<sup>71</sup> MURT is able to explain and make quantitative predictions about the translational energy, vibrational energy, rotational energy, and  $T_s$  dependence of  $S$ , as well as the isotope effect. However, the supersonic molecular beams used in the methane/Pt(111) experiments of Luntz and co-workers were rotationally cold, and their data does not directly allow any inferences to be made about the importance of rotational energy in the dissociative chemisorption of methane.

In this manuscript, we expand on the use of a three-parameter MURT and describe an alternative approach to obtaining and optimizing the required parameters that define the reactive transition state. An effusive molecular beam has well-defined vibrational, translational, and rotational energy distributions that allow us to probe the effects of all three molecular degrees of freedom on the dissociation dynamics. We measure dissociative sticking coefficients while specifying three experimental variables  $\vartheta$ ,  $T_g$ , and  $T_s$  of the effusive molecular beam experiments. By analyzing the data obtained with a MURT,<sup>57,58,75</sup> we obtain

three transition state parameters:  $s$  the effective number of surface oscillators involved in the collision complex,  $\nu_D$  a mean vibrational frequency, and  $E_0$  the threshold energy for reaction. The mean vibrational frequency represents a composite of four vibrational modes—three frustrated rotations as well as the vibration normal to the surface of the CH<sub>4</sub> molecule at the transition state. Consequently, by setting three experimental variables, we obtain three parameters that allow us to predict with startling accuracy<sup>57,58,70,71,73</sup> the dissociative sticking coefficients for arbitrary conditions, either equilibrium or nonequilibrium, quantum-state averaged or quantum-state resolved. This parameter set contains only one more element than an Arrhenius analysis, which has no predictive capacity for nonequilibrium or quantum-state-resolved measurements and significantly fewer than a catalog of error function parameters for each quantum state as necessitated by a dynamical model. Furthermore, the presence of strong and systematic deviations from MURT predictions—as opposed to random fluctuations—provides conclusive evidence for when kinetically relevant deviations from statistical behavior arise and lays a benchmark for determining when dynamical restrictions significantly affect reaction rates.

Our value of  $E_0$  can be compared directly with the results of electronic structure theory and the transition state barrier derived therefrom. In addition, MURT allows us to calculate the sticking coefficient dependence on any dynamical variable<sup>57,58,75</sup> and, hence, determine activation energies. For instance, we can calculate  $S$  as a function of  $T$  for a gas in equilibrium with the surface and thereby derive the thermal activation energy  $E_a$  appropriate to dissociative sticking in thermal bulb experiments.

In the MURT model,<sup>57,58,75</sup> we assume that CH<sub>4</sub> dissociation can be described microcanonically within the following scheme



The zero of energy  $E^*$  ( $= E_n + E_v + E_r + E_s$ ) occurs at 0 K with infinite separation between the surface and CH<sub>4</sub>. Methane incident on the surface forms a transient gas/surface collision complex consisting of the molecule and a few adjacent surface atoms. This local hot spot is an energetic, transient intermediate species, which is *not* in thermal equilibrium with the remainder of the substrate. Energy in this transiently formed physisorbed complex (PC or CH<sub>4(p)</sub> in eq 3) is assumed to be microcanonically randomized in an ensemble-averaged sense either through the collision process itself or through rapid intramolecular vibrational energy redistribution (IVR). A PC formed with total energy  $E^*$  subsequently either competitively desorbs or reacts with RRKM rate constants  $k_D(E^*)$  and  $k_R(E^*)$ . The ultrafast PC desorption rates ( $\tau_d \sim 2$  ps) at reactive energies lead to negligible energy exchange with the surrounding substrate.<sup>57,75</sup>

By applying the steady-state approximation to the coverage of CH<sub>4(p)</sub>, we obtain

$$S = \int_0^\infty S(E^*) f(E^*) dE^* \quad (4)$$

where

$$S(E^*) = \frac{W_R^\ddagger(E^* - E_0)}{W_R^\ddagger(E^* - E_0) + W_D^\ddagger(E^*)} \quad (5)$$

is the microcanonical sticking coefficient,  $W_i^\ddagger$  is the sum of states for transition state  $i$ ,  $E_0$  is the apparent threshold



energy for dissociation, and

$$f(E^*) = \int_0^{E^*} f_n(E_n) \int_0^{E^*-E_n} f_v(E_v) \int_0^{E^*-E_n-E_v} f_r(E_r) f_s(E^* - E_n - E_v - E_r) dE_r dE_v dE_n \quad (6)$$

is the flux distribution function for creating a physisorbed complex at  $E^*$ . One strength of the MURT analysis is that once the transition state characteristics have been defined by fits to experimental data or (in principle) by electronic structure theory calculations, the dependence of an experimental sticking coefficient for any dynamical variable ( $T_s$ ,  $E_n$ ,  $E_v$ , etc.) can be predicted on the basis of eq 4 by averaging the microcanonical sticking coefficient over the probability for creating a physisorbed complex at  $E^*$  under the specific experimental conditions of interest.

## Experimental Section

The Pt(111) crystal, oriented to within  $0.2^\circ$ , was cleaned using standard procedures involving  $\text{Ar}^+$  sputtering and annealing in  $\text{O}_2$ . Repeated cycles of  $\text{Ar}^+$  sputtering were performed at 800 K, oxidation at 800 K in an  $\text{O}_2$  atmosphere of  $5 \times 10^{-8}$  Torr, and annealing to 1250 K. Research purity methane (99.999%), ethane (99.995%), and CP grade ethylene (99.5%) were purchased from Matheson Tri-Gas and used without further purification. A lack of impurities was confirmed by mass spectrometry measured in the experimental apparatus with a doubly differentially ion pumped quadrupole mass spectrometer (QMS). This QMS was also used for temperature programmed desorption (TPD) measurements. Methane exposures were chosen in order to deposit  $\sim 0.04$ – $0.15$  ML C on the surface in any given run. The lower limit was selected so that activity at defect sites does not dominate (the particular Pt(111) crystal used has a defect density of  $\sim 0.002$  ML as determined by CO titration), and the upper limit was chosen in order to make our measurements an accurate approximation of the initial sticking coefficient. All coverages are reported in monolayers (ML) calculated with respect to the number of surface Pt atoms.

Carbon coverage was determined by Auger electron spectroscopy. To enhance the reproducibility and reliability of Auger electron spectroscopic determination of C coverage, all Auger data was collected at 500 K. This  $T_s$  ensured that any CO that may adventitiously adsorb during an experiment desorbed and that the decomposition of  $\text{CH}_x$  fragments to C was complete.<sup>76</sup> We recorded Auger spectra in integral mode from 200 to 300 eV using a 3 keV beam energy, encompassing both the  $\text{Pt}_{237}$  and  $\text{C}_{272}$  lines to lessen any differences in quantitation between carbidic and graphitic C. The program CasaXPS was used to perform a Shirley background subtraction on the interval from 210 to 280 eV and to fit the peaks to a mixed Gaussian/Lorentzian line shape.

The calibration of the absolute value of C coverage is somewhat problematic on Pt(111). The ambiguity stems from the fact that C can adopt either a carbidic or graphitic phase and that the phase depends on the thermal history of the sample. The carbidic phase has a saturation coverage at or below 1 ML, whereas the saturation coverage of the graphitic phase is much greater than 1 ML since the areal density of graphite is much greater than that of Pt. Furthermore, the phase of adsorbed C depends on  $T_s$  during adsorption and any subsequent annealing. The method of Biberian and Somorjai<sup>77</sup> requires prior knowledge of the saturation value of C atoms to Pt surface atoms to quantitatively specify the C coverage; otherwise it only yields a value relative to the unspecified areal density of C atoms in

a saturation layer. Therefore, we describe in some detail how we calibrated our Auger data.

Scanning tunneling microscope (STM) studies<sup>78</sup> have shown that graphite may be formed on Pt(111) by heating adsorbed ethylene. At 100 K, ethylene adsorbs molecularly to the surface, forming an ordered structure with a coverage of  $0.23 \pm 0.02$  ML, as determined by nuclear reaction studies<sup>79</sup> and supported by LEED analysis.<sup>80</sup> At 230 K, ethylene begins to convert irreversibly to ethylidyne ( $\text{CCH}_3$ ) by the loss of one hydrogen atom.<sup>81</sup> Between 430 and 700 K, the adsorbed ethylidyne undergoes further stepwise dehydrogenation, forming small islands of carbidic C on the surface. Annealing the surface above 800 K converts the carbidic islands to graphite. Graphite flows over steps in the Pt surface like a blanket, and therefore, the positioning of individual C atoms bears little relation to the underlying Pt lattice.<sup>78</sup> Monolayer graphite may also be formed on Pt(111) by exposure to alkane beams at high  $T_s$ .<sup>82</sup>

We used three methods to create saturated graphitic layers. First, ethylene was used in repeated cycles of dosing at 300 K then flashing to 1100 K to convert the adsorbed ethylidyne into graphite. The second and third methods involved exposure of the Pt(111) crystal at  $T_s = 1100$  K to a high flux of methane or ethane. In all three cases, stepwise Auger data were acquired and the C signal was found to saturate at a level that was identical within experimental uncertainty. This confirms that once a full monolayer was formed, no more ethylene, methane, or ethane adsorbed and that the saturation C coverage in all three cases was the same. Given the known areal density of a graphite layer ( $3.835 \times 10^{15} \text{ cm}^{-2}$ ) and the experimentally determined Auger intensity for that layer, we were able to calibrate our Auger signal quantitatively.

The main chamber was pumped by a  $210 \text{ l s}^{-1}$  turbomolecular pump, a  $240 \text{ l s}^{-1}$  ion pump, and a cryogenically cooled Ti sublimation pump (TSP). The base pressure was in the upper  $10^{-11}$  Torr range. The ion gauge, ion pump, and TSP filaments were turned off during dosing of the crystal to prevent alkanes from being cracked and forming potentially reactive radicals or ions. Gas pressure in the chamber was measured either with an ion gauge or with a bakeable Baratron (MKS model 615 with Type 670B signal conditioning electronics). Gas pressure in the gas handling manifold was measured with an MKS model 122B Baratron.

To exclude the possibility that some of the C deposited during the adsorption experiments originated from a source other than dissociative chemisorption of methane, several control experiments were performed. No C was detected by Auger when the Pt(111) surface was heated to 1100 K and exposed to  $10^{-2}$  Torr Ar for 10 min. Thus no C-containing contaminants were released from either the gas handling system or main vacuum chamber due to competitive adsorption, outgassing, or leaks. No C was detected by Auger when the Pt(111) crystal was heated to 1100 K and exposed to  $10^{-2}$  Torr CO or  $\text{CO}_2$  for 10 min. Thus, no C deposition resulted from decomposition of CO or  $\text{CO}_2$  emanating from background gas. No C deposition occurred when the Pt(111) surface, cooled to 100 K, was exposed to  $10^{-2}$  Torr  $\text{CH}_4$  for 10 min. This experiment eliminated the possibility of a high-sticking coefficient impurity in the gas bottle (such as ethylene) substantially contributing to the measured C deposition. Controls were also performed to ensure that  $\text{O}_2$  from the background gas was not removing deposited C from the surface.

The pressure during dosing was maintained low enough that no equilibration of the gas to  $T_s$  occurred. A lack of pressure

dependence in the sticking coefficients was confirmed for pressures below 1 Torr.

The effusive doser was heated by a W wire wrapped around a ceramic tube encasing the final 7.5 cm of the doser tubing. The temperature of the stainless steel tube never exceeded 700 K so as to avoid cracking of CH<sub>4</sub> within the nozzle; however, the W wire was heated to substantially higher temperatures. Control experiments indicated that the heated W wire did not result in an additional background contribution to the C deposition. When heated over the range of 400–700 K, the 0.05 cm diameter orifice in the doser increased by 0.65%, which resulted in a negligible change in the effusing gas flux.

Another phenomenon that could adversely affect the accuracy of dissociative sticking coefficient measurements is diffusion of C into the bulk of the Pt crystal. If such diffusion occurred, then the calculated sticking coefficients would be artificially low, since the amount of C measured by Auger would be smaller than the total amount of C deposited. On Ni(100),<sup>43</sup> significant C diffusion into the bulk begins above 475 K, and on Pt(110),<sup>83</sup> it begins above 1100 K. We found no data in the literature, however, on C diffusion into the bulk on the less reactive Pt(111) surface. Therefore, we performed a variety of experiments to investigate the effect of  $T_s$  and the phase of C, that is, graphitic vs carbidic, on diffusion of C into Pt(111).

Carbon was deposited on the surface either by dosing ethylene at 100 K followed by flashing to high temperature to dehydrogenate the adsorbed ethylene or by dissociative chemisorption of CH<sub>4</sub> at elevated  $T_s$ . When ethylene was dosed at low  $T_s$  and dehydrogenated by quickly flashing to 1100 K, the C formed was primarily carbidic. Depositing C by dissociative chemisorption of methane at 1100 K resulted in a mixture of carbidic and graphitic C, since rapid diffusion allowed by the high  $T_s$  permitted individual C atoms to “find” each other and begin forming graphite islands.<sup>78</sup> After an annealing procedure, Auger was used to determine if the C coverage had changed due to C diffusion into the bulk. The two different methods used to deposit C on the surface produce different initial states of C.

At temperatures up to 1100 K, both carbidic and graphitic C are stable on Pt(111) and do not diffuse into the bulk. Therefore, no depletion of C coverage is observed for C deposited either from C<sub>2</sub>H<sub>4</sub> dehydrogenation or from CH<sub>4</sub> dissociative chemisorption at  $T_s \leq 1100$  K. At 1200 K, carbidic C does diffuse into the bulk, while graphitic C does not. We find that, for CH<sub>4</sub> sticking experiments at  $T_s = 1200$  K, the surface coverage is minimally reduced by diffusion into the bulk because graphite formation competes favorably with bulk diffusion.

We report the sticking coefficient of methane incident on a Pt(111) crystal measured either (i) from a variable temperature molecular beam or (ii) from an isotropic ambient gas exposure. In both cases,  $T_s$  can be chosen arbitrarily in the range  $30 \text{ K} \leq T_s \leq 1200 \text{ K}$ . The temperature of the nozzle used to form the molecular beam was varied over the range  $295 \text{ K} \leq T_n \leq 680 \text{ K}$ . Time-of-flight measurements confirmed that the translational temperature of the molecules in the beam corresponded to the  $T_n$ . Because of the low pressure in experiments of type (2), which we refer to as angle-integrated experiments, the gas temperature was fixed at  $T_g = 295 \text{ K}$ .

The total carbon coverage on the surface is related to the incident flux by

$$\theta_{\text{C,total}} = S_{\text{eff}} \left( \frac{Z_{\text{W}} t}{\sigma_{\text{Pt}}} \right) \quad (7)$$

where  $S_{\text{eff}}$  is an effective sticking coefficient,  $Z_{\text{W}}$  is the flux

that is intercepted by the crystal,  $t$  the time, and  $\sigma_{\text{Pt}} = 1.50 \times 10^{15} \text{ cm}^{-2}$  is the areal density of Pt(111). For the molecular beam experiments, the value  $\theta_{\text{C,total}}$  must be corrected for a contribution due to molecules that have left the nozzle, bounced off of the crystal, and then equilibrated with the chamber walls before striking the crystal again. This background contribution was measured directly by turning the crystal away from the nozzle for nozzle temperatures  $295 \text{ K} \leq T_n \leq 680 \text{ K}$ . It can also be calculated by determining the sticking coefficient of 295 K gas and calculating the contribution resulting from the measured background pressure attained during an experiment. This correction was crucial because, for the lowest values of the sticking coefficient measured here, this background contribution can amount to up to half of the total C coverage. After subtracting the background contribution, the initial sticking coefficient was determined from

$$S = \frac{\theta_{\text{C}} \sigma_{\text{Pt}}}{Z_{\text{W}} t} \quad (8)$$

For the angle-integrated experiments, no background correction was required and  $S$  was determined directly from eq 8. In both cases,  $\theta_{\text{C}}$  was kept low enough that we need not consider the effect of coverage on the sticking coefficient. This assumption was checked by direct measurement of the C uptake curve due to progressively higher exposure of CH<sub>4</sub> at elevated  $T_s$ , which eventually led to saturation of the surface. These measurements confirmed that all reported values of the sticking coefficient correspond to the coverage region in which the coverage is linearly dependent on the exposure.

To characterize the degree of agreement between the predictions of the MURT analysis (theory) and experimental data (exp), we introduce the average relative discrepancy as defined by

$$\text{ARD} = \left\langle \frac{|S_{\text{theory}} - S_{\text{exp}}|}{\min(S_{\text{theory}}, S_{\text{exp}})} \right\rangle \quad (9)$$

## Results

Previously,<sup>57</sup> a MURT analysis was used to fit the supersonic molecular beam results of Luntz and co-workers.<sup>50,51</sup> This analysis, however, did not use ARD to quantify the goodness of fit. Recalculating the fit and using the ARD to quantify when the parameters are optimized, we arrive at  $\{E_0 = 56 \text{ kJ mol}^{-1}, s = 3, \nu_{\text{D}} = 125 \text{ cm}^{-1}\}$  with an ARD of 34%. This parameter set differs slightly from that obtained before  $\{E_0 = 59 \text{ kJ mol}^{-1}, s = 3, \nu_{\text{D}} = 110 \text{ cm}^{-1}\}$  but does provide an improved fit (ARD of 34% vs 38%) compared with that shown in Figures 3 and 4 of ref 57. The results for both our effusive molecular beam and angle-integrated experiments are presented in Figure 1. Also presented in Figure 1 are solid lines, which depict the predicted values of  $S$  derived from the MURT analysis for the effusive molecular beam experiments, and a dashed line, which depicts the MURT prediction for the angle-integrated data. Optimization of the MURT parameters relative to our molecular beam data resulted in an ARD of 41% and an optimized parameter set of  $\{E_0 = 49 \text{ kJ mol}^{-1}, s = 2, \nu_{\text{D}} = 330 \text{ cm}^{-1}\}$ . This optimized parameter set also yields a very satisfying fit of the room-temperature angle-integrated sticking data. The thermal sticking coefficient appropriate to angle-integrated experiments with  $T = T_g = T_s$  at room temperature was measured as  $S_{\text{T}}(295 \text{ K}) = 1.65 \times 10^{-10}$ , which compares well with the PC-MURT prediction of  $1.45 \times 10^{-10}$  (ARD = 14%).

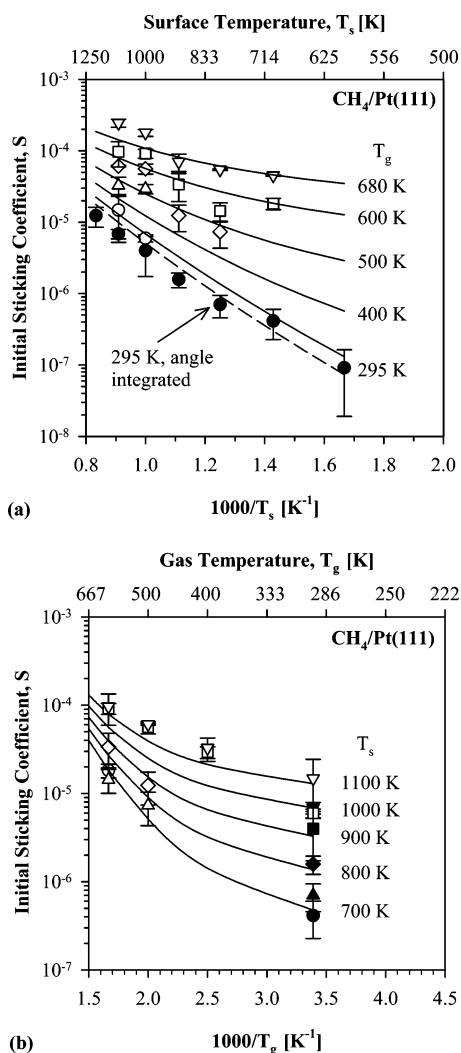


**Figure 1.** Initial dissociative sticking coefficient  $S$  is plotted vs the inverse of (a) surface temperature,  $T_s$ , and (b) gas temperature,  $T_g$ . Filled symbols refer to the angle-integrated data from ambient gas dosing at  $T_g = 295$  K. Open symbols correspond to the effusive molecular beam experiments where the nozzle temperature is taken to specify  $T_g$ . PC-MURT predictions for the angle-integrated (dashed line) and effusive molecular beam (solid lines) data are indicated. For clarity, single measurements at  $T_s = 600$  and  $1200$  K appearing in (a) are not replotted in (b).

Comparisons of quantitative kinetics data are notoriously fraught with difficulties in absolute calibration of surface experiments. An order of magnitude or more variation in absolute rates or dissociative sticking coefficients is not uncommon.<sup>1</sup> When we compare the results of the two independent fits (supersonic molecular beam vs effusive molecular beam), we find that both sets capture the general shapes of the other set. All trends are reproduced. However, a rigid shift by a factor of about 8.5 is required to make the data sets overlap. Therefore, within the range of possible calibration errors, the reported sets of fit parameters should be treated as most probable bounds on the individual values. Hence,  $\{E_0 = 52.5 \pm 3.5 \text{ kJ mol}^{-1}, s = 2-3, \nu_D = 227.5 \pm 102.5 \text{ cm}^{-1}\}$ . As we shall see in the comparison to previous values of  $E_0$  below, this represents a significant advance in defining the value of  $E_0$ , even though there is still uncertainty within a factor of 8.5 in the absolute value of the sticking coefficient as determined by experiment.

We can now compare to prior results for the  $\text{CH}_4/\text{Pt}(111)$   $E_0$  derived from electronic structure theory and experiments.  $E_0 = 81 \text{ kJ mol}^{-1}$  was predicted by Au et al.<sup>84</sup> and  $64 \text{ kJ mol}^{-1}$  by

Michaelides and Hu<sup>85</sup> from density functional calculations on small Pt clusters. Anderson and Maloney<sup>86</sup> calculated  $E_0 = 43 \text{ kJ mol}^{-1}$  with the atom superposition and electron delocalization molecular orbital method. Shustorovich and Sellers<sup>87</sup> calculated  $75 \text{ kJ mol}^{-1}$  with a bond-order conservation Morse potential method. Previous experimental estimates of the barrier height ( $121 \text{ kJ mol}^{-1}$ , ref 88, and  $244 \text{ kJ mol}^{-1}$ , ref 89) were derived from models based on tunneling. Since tunneling is not the primary means of barrier crossing, we disregard these estimates.

## Discussion

The PC-MURT analysis describes the results of dissociative chemisorption experiments with an accuracy of roughly 34–41%. The parameters derived from this analysis are  $\{E_0 = 52.5 \pm 3.5 \text{ kJ mol}^{-1}, s = 2-3, \nu_D = 227.5 \pm 102.5 \text{ cm}^{-1}\}$ . The measured barrier height falls within the considerable scatter of values derived on the basis of electronic structure theory calculations and it would appear that significant improvement could be made in these calculations.

Luntz and Harris<sup>46–50</sup> developed a reduced dimensionality, quantum mechanical model that incorporates surface motion and allows for tunneling in dissociation. They have argued that this model of thermally assisted tunneling (TAT) can account for all available dissociative chemisorption data. Figure 2 compares the ability of the PC-MURT and TAT to match experimental data. While it should be noted that Harris et al. did not attempt to fit their model for quantitative agreement, nevertheless, the ARD for their  $\text{CH}_4$  predictions in Figure 2c is 2793% (cf., the PC-MURT's 34% ARD for all the experimental data). While the generally decreasing value of  $S$  with decreasing  $T_s$  is confirmed in their model, the agreement is not overwhelming regarding the slope of the dependence. This is particularly true when one realizes that the TAT lines in Figure 2d are calculated for normal translational energies that are much different than the values of  $E_n$  for the experimental data points that lie nearest to each TAT curve. Furthermore, Figure 2c demonstrates unequivocally that TAT does not properly predict the dependence of  $\text{CH}_4$  and  $\text{CD}_4$  on  $E_n$ . TAT does not reproduce the isotope effect in dissociative chemisorption of methane, whereas Figure 2a demonstrates unambiguously that the PC-MURT correctly describes the isotope effect. Similarly good treatment of the kinetic isotope effect by the PC-MURT is seen for methane dissociation on  $\text{Ni}(100)$ .<sup>58,70,71</sup> Since tunneling is not involved in the PC-MURT model, we can rule out the significance of tunneling in the dissociation of methane on  $\text{Pt}(111)$ .

Because of its superior predictive capacity and ability to address all aspects of the dependence of  $S$  on dynamical parameters, including the isotope effect,<sup>57</sup> we believe that the MURT contains the essence of the dissociation dynamics. Furthermore, its combination with the data from angle-integrated and effusive molecular beam measurements gives us insight into the dissociative chemisorption dynamics for equilibrium as well as nonequilibrium conditions. Molecular beams have the advantages of being able to vary the beam energy independent of  $T_s$  and of significantly increasing  $S$  to a high information content regime. With an effusive beam, we are able to access the effects of all molecular degrees of freedom—including rotation—as well as the surface temperature. With MURT analysis, we are able to deconvolute the importance of each degree of freedom in the dissociation dynamics.<sup>57,58,75</sup> By combining the two, we are able to perform this deconvolution without the need to perform molecular beam experiments for each individual quantum state. While such extensive measure-



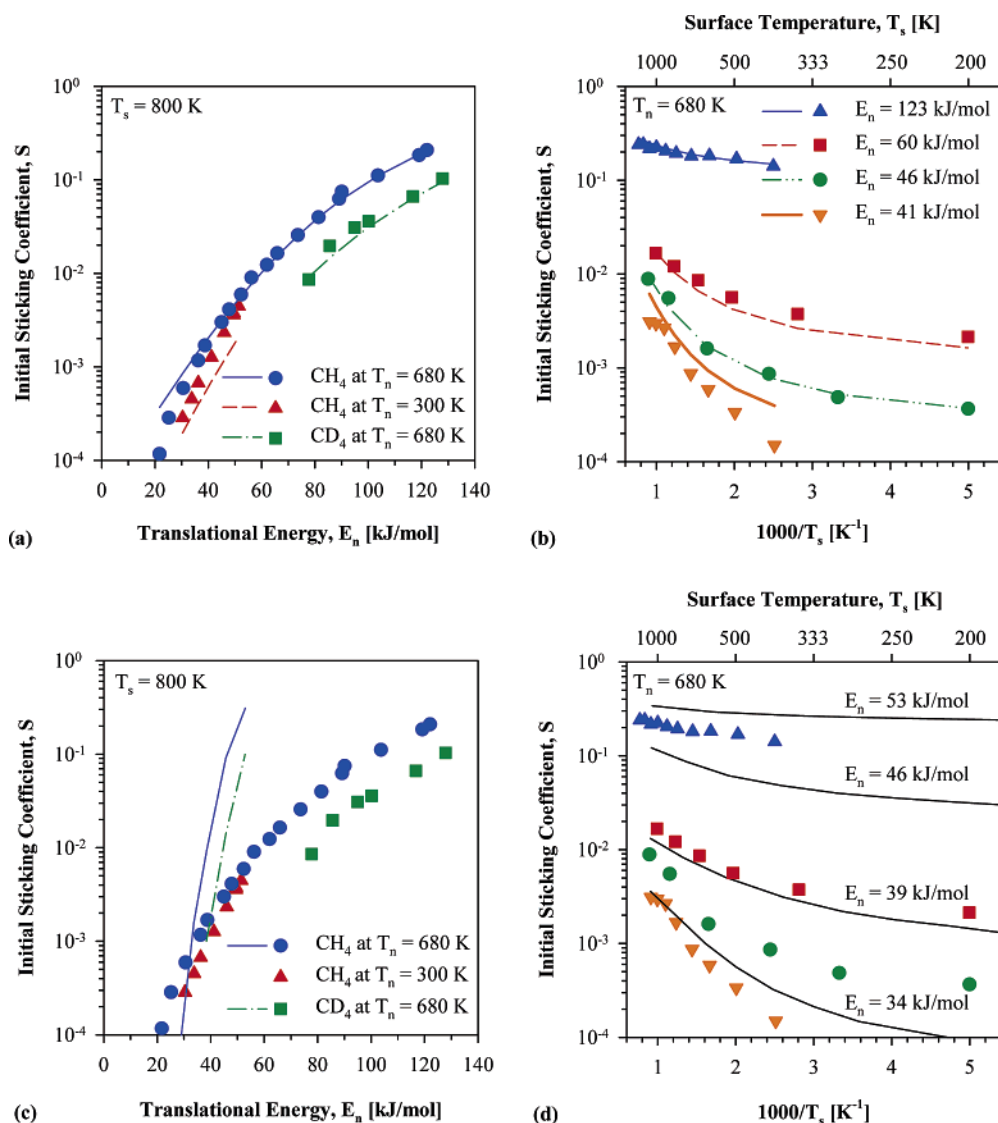


**Figure 2.** Comparison of the methane/Pt(111) supersonic molecular beam experiments of ref 50 (solid points) to the predictions of the PC-MURT (lines of (a) and (b)) and the thermally assisted tunneling (TAT) model<sup>50</sup> (lines of (c) and (d)). (a) PC-MURT correctly accounts for the mean normal translational energy,  $E_n$ , molecular beam nozzle temperature,  $T_n$ , and isotope dependence of the dissociative sticking. (b) PC-MURT accurately predicts the  $T_s$  dependence of the dissociative sticking. (c) TAT does not correctly predict the magnitude of dissociative sticking nor its dependence on  $E_n$  or the isotope. (d) Despite initial appearances, TAT does not accurately predict the  $T_s$  dependence of the dissociative sticking because the TAT lines are calculated for  $E_n$  values very different from those of the nearby experimental points (see the legend of (b) for the experimental  $E_n$  values).

ments may be feasible for H<sub>2</sub>,<sup>90</sup> over 1400 vibrational states must be considered to describe the thermal sticking of CH<sub>4</sub> at  $T_s = 1000$  K.<sup>58</sup> The pragmatic advantage of combining effusive molecular beam data with MURT analysis is apparent.

Previous work<sup>9–14,91</sup> has suggested a degree of mode specificity in the dissociation of methane on Ni surfaces but has been unable to ascertain its relevance to thermally state-averaged kinetics. For instance, the excitation of the antisymmetric stretch  $\nu_3$  enhances reactivity more efficiently than translation on Ni(111), but the excitation of the  $3\nu_4$  level is less efficient even though it lies at higher energy. Such results have led to statements such as “statistical models cannot correctly describe the chemisorption of CH<sub>4</sub>”<sup>14</sup> which is certainly true if “correctly” means to “completely” describe all the molecular details of the chemisorption dynamics on the 15–16 dimensional reactive potential energy surface that must be further coupled to the surrounding surface heat bath. On the other hand, the three-parameter, full dimensionality PC-MURT approximation has proven capable of quantitatively predicting the dissociative chemisorption of CH<sub>4</sub> on Ni(100)<sup>58,71</sup> and Ir(111)<sup>72</sup> for diverse

experiments spanning some 9 orders of magnitude in sticking coefficient and 10 orders in pressure. Similarly, we find that the PC-MURT successfully predicts dissociative sticking coefficients for the CH<sub>4</sub>/Pt(111) system.

The PC-MURT is able to characterize the results from our experiments performed at thermal equilibrium or for  $T_s \neq T_g$ , in either a thermally averaged or quantum-state-resolved manner.<sup>58,75</sup> The calculated sticking coefficients differ from our effusive beam data on average by 41% for  $295 \text{ K} \leq T_s \leq 1200 \text{ K}$  and  $295 \leq T_g \leq 680 \text{ K}$ . While the details of the dissociation reaction may require a dynamical description in which some specific modes are more important than others, when looking at the overall kinetic process for an ensemble of molecules interacting with a metal surface, much of these quantum state variations may average out and a statistical approach provides a good description of the mean chemical interaction and the overall dynamics. Furthermore, the success of the “over-the-barrier” MURT precludes an important role for tunneling in the dissociative chemisorption of methane under ordinary experimental conditions.

Dating back to the early work of Winters,<sup>15,16</sup> and Ehrlich and co-workers,<sup>18–20</sup> much debate has centered on the relative roles of molecular excitations vs surface excitations in the activation of CH<sub>4</sub> over metal surfaces. What the MURT analysis shows is that all of the molecular degrees of freedom as well as  $T_s$  are important for determining the dissociation probability. Furthermore, the role of a particular degree of freedom in determining  $S$  varies with the energy distributions of the specific experiment. (e.g., see eqs 4 and 6). In the supersonic molecular beam experiments of Figure 2b, if the mean translational energy is already near or well in excess of the dissociation threshold energy (52.5 kJ/mol), then the relative importance of the surface temperature is reduced. At lower mean translational energies, the sensitivity of  $S$  to the surface temperature is increased because of the greater need to draw energy from the surface in order to attain a pooled PC total energy sufficient to react. Similarly for the effusive beams, the dependence of sticking on  $T_s$  becomes less dramatic for increasing  $T_g$ , as seen in Figure 1a. Likewise, the sensitivity of  $S$  to  $T_g$  decreases with increasing  $T_s$ , as seen in Figure 1b. These trends are consistent with the experiments of Luntz and Bethune on Pt(111)<sup>51</sup> and Luntz and Winters on Pt(100).<sup>52</sup>

Frequently, any sign of a  $T_s$  dependence has been taken to be evidence for precursor mediated adsorption. The thermally assisted tunneling model<sup>46–50</sup> demonstrated that this need not be the case, and in this respect, the MURT agrees. Note that the MURT comes to this conclusion without invoking any form of tunneling dynamics, which, upon later reflection,<sup>92</sup> does not seem to be that important for barrier crossing even within the thermally assisted tunneling model. In the PC-MURT, the initial thermal energy of the local cluster of surface atoms involved in the collision complex can be pooled with the active molecular energy to aid in passage over the transition state barrier. It is through this over-the-barrier path, rather than through the effects of tunneling, that  $T_s$  affects  $S$ .

Our results are not influenced by steps for the coverage range 0.04–0.15 ML, for which we find a linear relationship between exposure and coverage. This is not inconsistent with the measurements of Gee et al.<sup>93</sup> in that it appears that C atoms are immobilized at the step. From the work of Egeberg et al.<sup>94</sup> on Ni(111) and Ru(0001), it does not appear that steps and defects are particularly more active than terrace sites, especially if a small coverage of C is allowed to build up as is the case for our measurements.

In light of the apparently minor role of defects in determining the dissociation dynamics of CH<sub>4</sub> on metal surfaces, it is interesting to compare our results with those derived from experiments on dispersed nanoclusters of Pt on oxide substrates. These steam and dry reforming catalysts have been studied extensively by Wei and Iglesia<sup>95</sup> under thermal equilibrium and at high pressure. Their steady-state reaction rates on a per exposed metal atom basis for a 1.6 wt % Pt/ZrO<sub>2</sub> catalyst (~2 nm diam Pt nanoclusters) are plotted in Figure 3 along with the predictions of the PC-MURT for Pt(111). The data exhibit comparable effective activation energies. Wei and Iglesia report 78 kJ mol<sup>-1</sup>. We observe some curvature in the ln  $S$  vs  $1/T$  data, but using the same temperature range, we calculate a thermal activation energy in the range 60 kJ mol<sup>-1</sup> ≤  $E_a$  ≤ 68 kJ mol<sup>-1</sup>. As expected  $E_a$  exceeds  $E_0$ . Somewhat surprisingly, the reactivity of the smooth, flat Pt(111) single-crystal surface exceeds that of the nanoscale Pt clusters dispersed on ZrO<sub>2</sub> by over 2 orders of magnitude even though smaller clusters, which presumably expose a greater fraction of coordinatively unsaturated surface Pt atoms than flat surfaces, have been shown to

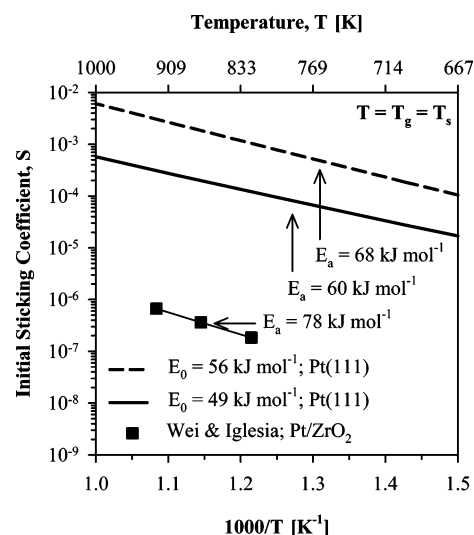


**Figure 3.** Comparison of the high-pressure thermal reactivity of CH<sub>4</sub> over a supported Pt nanocatalyst from ref 95 with the thermal predictions of the PC-MURT for CH<sub>4</sub>/Pt(111) using (i) the Figure 1 parameter set of  $\{E_0 = 49 \text{ kJ mol}^{-1}, s = 2, \nu_D = 330 \text{ cm}^{-1}\}$  (solid line) and (ii) the parameter set derived from the supersonic molecular beam data of Luntz and Bethune  $\{E_0 = 56 \text{ kJ mol}^{-1}, s = 3, \nu_D = 125 \text{ cm}^{-1}\}$  (dashed line).

be more reactive than bigger clusters.<sup>96</sup> A similar superiority for the reactivity of a single crystal compared with high-surface-area catalysts was observed for Ni.<sup>42,43,45</sup> A likely explanation for this finding is that at steady state, C plays a role in deactivating the catalyst. Wei and Iglesia were very careful to measure reaction rates on a per exposed Pt surface atom basis and were able to rule out any build over coverage of unreactive species. Therefore, the deactivation of the nanocatalysts may involve both C atoms *absorbed* in the *subsurface* region and C atoms *adsorbed* on the surface. On the optimistic side, however, this points toward a possibility for substantial improvement in the reactivity of industrial reforming catalysts if a method for suppressing the deactivation can be found.

## Conclusions

For a polyatomic molecule such as CH<sub>4</sub>, it is impossible to measure individual sticking coefficients for all quantum states relevant to thermal sticking. With a combination of micro-canonical unimolecular rate theory (MURT) and an effusive molecular beam, we access all of these states and, more importantly, we can deconvolute their dynamical relevance.<sup>57,58,75</sup> We have demonstrated the ability of the MURT analysis to quantitatively describe nonequilibrium dissociation data for CH<sub>4</sub>/Pt(111), regardless of whether dissociation results from exposure to a supersonic or effusive molecular beam or from an ambient thermal gas. Thus, even if there are some mode-specific corrections to the dissociative sticking for individual quantum states, these are not of great kinetic significance either because they are not large or because they compensate for one another. Neither is tunneling found to be important for dissociation. The dynamics of CH<sub>4</sub> dissociation on Pt(111) are essentially described by an over-the-barrier process, competitive with desorption, in which the determining factor is the total active energy of the complex that is formed when a CH<sub>4</sub> molecule interacts with two to three surface atoms upon collision. Consistent with this picture, the surface temperature as well as the translational, vibrational and rotational excitations of the molecule are all important in determining the dissociative sticking coefficient and overcoming a dissociation threshold energy of  $52.5 \pm 3.5 \text{ kJ mol}^{-1}$ .



**Acknowledgment.** This research was supported by the National Science Foundation (NSF) Grant No. 0415540, the donors of the American Chemical Society Petroleum Research Fund, and the University of Virginia. K.M.D., L.V., and H.L.A. gratefully acknowledge fellowship support under NSF IGERT Grant No. 9972790.

## References and Notes

- (1) Larsen, J. H.; Chorkendorff, I. *Surf. Sci. Rep.* **1999**, *35*, 163.
- (2) Labinger, J. A.; Bercaw, J. E. *Nature* **2002**, *417*, 507.
- (3) Choudhary, T. V.; Aksoylu, E.; Goodman, D. W. *Catal. Rev.* **2003**, *45*, 151.
- (4) Kolasinski, K. W. *Surface Science: Foundations of Catalysis and Nanoscience*; John Wiley & Sons: Chichester, U.K., 2002.
- (5) Comsa, G.; David, R. *Surf. Sci. Rep.* **1985**, *5*, 145.
- (6) Kleyn, A. W. *Chem. Soc. Rev.* **2003**, *32*, 87.
- (7) Hodgson, A. *Prog. Surf. Sci.* **2000**, *63*, 1.
- (8) Weaver, J. F.; Carlsson, A. F.; Madix, R. J. *Surf. Sci. Rep.* **2003**, *50*, 107.
- (9) Juurlink, L. B. F.; McCabe, P. R.; Smith, R. R.; DiCologero, C. L.; Utz, A. L. *Phys. Rev. Lett.* **1999**, *83*, 868.
- (10) Juurlink, L. B. F.; Smith, R. R.; Killelea, D. R.; Utz, A. L. *Phys. Rev. Lett.* **2005**, *94*, 208303.
- (11) Smith, R. R.; Killelea, D. R.; DelSesto, D. F.; Utz, A. L. *Science* **2004**, *304*, 992.
- (12) Schmid, M. P.; Maroni, P.; Beck, R. D.; Rizzo, T. R. *J. Chem. Phys.* **2002**, *117*, 8603.
- (13) Beck, R. D.; Maroni, P.; Papageorgopoulos, D. C.; Dang, T. T.; Schmid, M. P.; Rizzo, T. R. *Science* **2003**, *302*, 98.
- (14) Maroni, P.; Papageorgopoulos, D. C.; Sacchi, M.; Dang, T. T.; Beck, R. D.; Rizzo, T. R. *Phys. Rev. Lett.* **2005**, *94*, 246104.
- (15) Winters, H. F. *J. Chem. Phys.* **1975**, *62*, 2454.
- (16) Winters, H. F. *J. Chem. Phys.* **1976**, *64*, 3495.
- (17) Rettner, C. T.; Pfnür, H. E.; Auerbach, D. J. *Phys. Rev. Lett.* **1985**, *54*, 2716.
- (18) Brass, S. G.; Ehrlich, G. *Phys. Rev. Lett.* **1986**, *57*, 2532.
- (19) Stewart, C. N.; Ehrlich, G. *J. Chem. Phys.* **1975**, *62*, 4672.
- (20) Ehrlich, G. Activated Chemisorption. In *Chemistry and Physics of Solid Surfaces VII*; Vanselow, R., Howe, R. F., Eds.; Springer-Verlag: New York, 1988; Vol. 10, p 1.
- (21) Lo, T.-C.; Ehrlich, G. *Surf. Sci.* **1987**, *179*, L19.
- (22) Hamza, A. V.; Madix, R. J. *Surf. Sci.* **1987**, *179*, 25.
- (23) Hamza, A. V.; Steinrück, H.-P.; Madix, R. J. *J. Chem. Phys.* **1987**, *86*, 6506.
- (24) Arumainayagam, C. R.; McMaster, M. C.; Schoofs, G. R.; Madix, R. J. *Surf. Sci.* **1989**, *222*, 213.
- (25) Kao, C.-L.; Madix, R. J. *Surf. Sci.* **2004**, *557*, 215.
- (26) Yates, J. T., Jr.; Zinck, J. J.; Sheard, S.; Weinberg, W. H. *J. Chem. Phys.* **1979**, *70*, 2266.
- (27) Szuromi, P. D.; Engstrom, J. R.; Weinberg, W. H. *J. Chem. Phys.* **1984**, *80*, 508.
- (28) Szuromi, P. D.; Weinberg, W. H. *Surf. Sci.* **1985**, *149*, 226.
- (29) Weinberg, W. H. Kinetics of Surface Reactions. In *Dynamics of Gas-Surface Interactions*; Rettner, C. T., Ashfold, M. N. R., Eds.; The Royal Society of Chemistry: Cambridge, U.K., 1991; p 171.
- (30) Johnson, D. F.; Weinberg, W. H. *Science* **1993**, *261*, 76.
- (31) Weinberg, W. H. *J. Vac. Sci. Technol., A* **1992**, *10*, 2271.
- (32) Verhoef, R. W.; Kelly, D.; Mullins, C. B.; Weinberg, W. H. *Surf. Sci.* **1993**, *291*, L719.
- (33) Weinberg, W. H. *Langmuir* **1993**, *9*, 655.
- (34) Seets, D. C.; Wheeler, M. C.; Mullins, C. B. *Chem. Phys. Lett.* **1997**, *266*, 431.
- (35) Seets, D. C.; Wheeler, M. C.; Mullins, C. B. *J. Chem. Phys.* **1997**, *107*, 3986.
- (36) Seets, D. C.; Reeves, C. T.; Ferguson, B. A.; Wheeler, M. C.; Mullins, C. B. *J. Chem. Phys.* **1997**, *107*, 10229.
- (37) Beckerle, J. D.; Yang, Q. Y.; Johnson, A. D.; Ceyer, S. T. *J. Chem. Phys.* **1987**, *86*, 7236.
- (38) Lee, M. B.; Yang, Q. Y.; Ceyer, S. T. *J. Chem. Phys.* **1987**, *87*, 2724.
- (39) Beckerle, J. D.; Johnson, A. D.; Yang, Q. Y.; Ceyer, S. T. *J. Chem. Phys.* **1989**, *91*, 5756.
- (40) Beckerle, J. D.; Johnson, A. D.; Ceyer, S. T. *Phys. Rev. Lett.* **1989**, *62*, 685.
- (41) Campbell, R. A.; Szanyi, J.; Lenz, P.; Goodman, D. W. *Catal. Lett.* **1993**, *17*, 39.
- (42) Beebe, T. P., Jr.; Goodman, D. W.; Kay, B. D.; Yates, J. T., Jr. *J. Chem. Phys.* **1987**, *87*, 2305.
- (43) Holmblad, P. M.; Wambach, J.; Chorkendorff, I. *J. Chem. Phys.* **1995**, *102*, 8255.
- (44) Larsen, J. H.; Holmblad, P. M.; Chorkendorff, I. *J. Chem. Phys.* **1999**, *110*, 2637.
- (45) Nielsen, B. Ø.; Luntz, A. C.; Holmblad, P. M.; Chorkendorff, I. *Catal. Lett.* **1995**, *32*, 15.
- (46) Harris, J.; Luntz, A. C. *Surf. Sci.* **1993**, *287*–288, 56.
- (47) Luntz, A. C.; Harris, J. *J. Chem. Phys.* **1992**, *96*, 7054.
- (48) Luntz, A. C.; Harris, J. *J. Vac. Sci. Technol., A* **1992**, *10*, 2292.
- (49) Luntz, A. C.; Harris, J. *Surf. Sci.* **1991**, *258*, 397.
- (50) Harris, J.; Simon, J.; Luntz, A. C.; Mullins, C. B.; Rettner, C. T. *Phys. Rev. Lett.* **1991**, *67*, 652.
- (51) Luntz, A. C.; Bethune, D. S. *J. Chem. Phys.* **1989**, *90*, 1274.
- (52) Luntz, A. C.; Winters, H. F. *J. Chem. Phys.* **1994**, *101*, 10980.
- (53) Walker, A. V.; King, D. A. *Phys. Rev. Lett.* **1999**, *82*, 5156.
- (54) Anghel, A. T.; Wales, D. J.; Jenkins, S. J.; King, D. A. *Phys. Rev. B* **2005**, *71*, 113410.
- (55) Ukraintsev, V. A.; Harrison, I. *J. Chem. Phys.* **1994**, *101*, 1564.
- (56) Higgins, J.; Conjusteau, A.; Scoles, G.; Bernasek, S. L. *J. Chem. Phys.* **2001**, *114*, 5277.
- (57) Bukoski, A.; Blumling, D.; Harrison, I. *J. Chem. Phys.* **2003**, *118*, 843.
- (58) Abbott, H. L.; Bukoski, A.; Harrison, I. *J. Chem. Phys.* **2004**, *121*, 3792.
- (59) Nielson, B. Ø.; Polanyi, J. C. *Acc. Chem. Res.* **1972**, *5*, 161.
- (60) Polanyi, J. C.; Wong, W. H. *J. Chem. Phys.* **1969**, *51*, 1439.
- (61) Mok, M. H.; Polanyi, J. C. *J. Chem. Phys.* **1969**, *51*, 1451.
- (62) Zare, R. N. *Science* **1998**, *279*, 1875.
- (63) Crim, F. F. *Acc. Chem. Res.* **1999**, *32*, 877.
- (64) Kim, Z. H.; Bechtel, H. A.; Zare, R. N. *J. Am. Chem. Soc.* **2001**, *123*, 12714.
- (65) Yoon, S.; Holiday, R. J.; Sibert, E. L., III; Crim, F. F. *J. Chem. Phys.* **2003**, *119*, 9568.
- (66) Rettner, C. T.; DeLouise, L. A.; Auerbach, D. J. *J. Chem. Phys.* **1986**, *85*, 1131.
- (67) Harris, J. *Surf. Sci.* **1989**, *221*, 335.
- (68) Michelsen, H. A.; Rettner, C. T.; Auerbach, D. J.; Zare, R. N. *J. Chem. Phys.* **1993**, *98*, 8294.
- (69) Luntz, A. C. *J. Chem. Phys.* **2000**, *113*, 6901.
- (70) Bukoski, A.; Harrison, I. *J. Chem. Phys.* **2003**, *118*, 9762.
- (71) Abbott, H. L.; Bukoski, A.; Kavulak, D. F.; Harrison, I. *J. Chem. Phys.* **2003**, *119*, 6407.
- (72) Abbott, H. L.; Harrison, I. *J. Phys. Chem. B* **2005**, *109*, 10371.
- (73) Kavulak, D. F.; Abbott, H. L.; Harrison, I. *J. Phys. Chem. B* **2005**, *109*, 685.
- (74) See ref 45.
- (75) Bukoski, A.; Abbott, H. L.; Harrison, I. *J. Chem. Phys.* **2005**, *123*, 094707.
- (76) Fuhrmann, T.; Kinne, M.; Whelan, C. M.; Zhu, J. F.; Denecke, R.; Steinrück, H.-P. *Chem. Phys. Lett.* **2003**, *390*, 208.
- (77) Biberian, J. P.; Somorjai, G. A. *Appl. Surf. Sci.* **1979**, *2*, 352.
- (78) Land, T. A.; Michely, T.; Behm, R. J.; Hemminger, J. C.; Comsa, G. *J. Chem. Phys.* **1992**, *97*, 6774.
- (79) Mitchell, I. V.; Lennard, W. N.; Griffiths, K.; Massoumi, G. R.; Huppertz, J. W. *Surf. Sci.* **1991**, *256*, L598.
- (80) Starke, U.; Barbieri, A.; Materer, N.; Van Hove, M. A.; Somorjai, G. A. *Surf. Sci.* **1993**, *286*, 1.
- (81) Somorjai, G. A.; McCrea, K. R. Dynamics of reactions at surfaces. In *Advances in Catalysis*; Gates, B. C., Knözinger, H., Eds.; Academic Press: Boston, MA, 2000; Vol. 45, pp 386–438.
- (82) Ueta, H.; Saida, M.; Nakai, C.; Yamada, Y.; Sasaki, M.; Yamamoto, S. *Surf. Sci.* **2004**, *560*, 183.
- (83) Boronin, A. I.; Bukhtiyarov, V. I.; Kvon, R.; Chesnokov, V. V.; Buyanov, R. A. *Surf. Sci.* **1991**, *258*, 289.
- (84) Au, C.-T.; Ng, C.-F.; Liao, M.-S. *J. Catal.* **1999**, *185*, 12.
- (85) Michaelides, A.; Hu, P. *J. Am. Chem. Soc.* **2000**, *122*, 9866.
- (86) Anderson, A. B.; Maloney, J. J. *J. Phys. Chem.* **1988**, *92*, 809.
- (87) Shustorovich, E.; Sellers, H. *Surf. Sci. Rep.* **1998**, *31*, 1.
- (88) Schoofs, G. R.; Arumainayagam, C. R.; McMaster, M. C.; Madix, R. J. *Surf. Sci.* **1989**, *215*, 1.
- (89) Valden, M.; Pere, J.; Hirsimäki, M.; Suhonen, S.; Pessa, M. *Surf. Sci.* **1997**, *377*, 605.
- (90) Rettner, C. T.; Michelsen, H. A.; Auerbach, D. J. *Faraday Discuss. Chem. Soc.* **1993**, *96*, 17.
- (91) Juurlink, L. B. F.; Smith, R. R.; Utz, A. L. *Faraday Discuss. Chem. Soc.* **2000**, *117*, 147.
- (92) Luntz, A. C. *J. Chem. Phys.* **1995**, *102*, 8264.
- (93) Gee, A. T.; Hayden, B. E.; Mormiche, C.; Kleyn, A. W.; Riedmüller, B. *J. Chem. Phys.* **2003**, *118*, 3334.
- (94) Egeberg, R. C.; Ullmann, S.; Alstrup, I.; Mullins, C. B.; Chorkendorff, I. *Surf. Sci.* **2002**, *497*, 183.
- (95) Wei, J.; Iglesia, E. *J. Phys. Chem. B* **2004**, *108*, 4094.
- (96) Ramallo-Lopez, M. A.; Requejo, F. G.; Craievich, A. F.; Wei, J.; Avalos-Borja, M.; Iglesia, E. *J. Mol. Catal. A: Chem.* **2005**, *228*, 299.